

## Sensitivity of the Indian Monsoon to Human Activities

B. KNOPF<sup>\*1</sup>, K. ZICKFELD<sup>2</sup>, M. FLECHSIG<sup>1</sup>, and V. PETOUKHOV<sup>1</sup>

<sup>1</sup>*Potsdam Institute for Climate Impact Research (PIK), PO Box 60 12 03, 14412 Potsdam, Germany*

<sup>2</sup>*School of Earth and Ocean Sciences, University of Victoria, Victoria, BC, Canada*

(Received 30 May 2007; revised 29 February 2008)

### ABSTRACT

In this paper the authors perform an extensive sensitivity analysis of the Indian summer monsoon rainfall to changes in parameters and boundary conditions which are influenced by human activities. For this study, the authors use a box model of the Indian monsoon which reproduces key features of the observed monsoon dynamics such as the annual course of precipitation and the transitions between winter and summer regimes. Because of its transparency and computational efficiency, this model is highly suitable for exploring the effects of anthropogenic perturbations such as emissions of greenhouse gases and sulfur dioxide, and land cover changes, on the Indian monsoon.

Results of a systematic sensitivity analysis indicate that changes in those parameters which are related to emissions of greenhouse gases lead to an increase in Indian summer rainfall. In contrast, all parameters related to higher atmospheric aerosol concentrations lead to a decrease in Indian rainfall. Similarly, changes in parameters which can be related to forest conversion or desertification, act to decrease the summer precipitation. The results indicate that the sign of precipitation changes over India will be dependent on the direction and relative magnitude of different human perturbations.

**Key words:** Indian monsoon, sensitivity analysis, global change, anthropogenic climate change

**Citation:** Knopf, B, K. Zickfeld, M. Flechsig, and V. Petoukhov, 2008: Sensitivity of the Indian monsoon to human activities. *Adv. Atmos. Sci.*, **25**(6), 932–945, doi: 10.1007/s00376-008-0932-5.

---

### 1. Introduction

The Indian Monsoon is an annual recurring phenomenon that brings vital rain to India. Life in India depends strongly on the monsoon rain and its effects on India's agriculture (Parthasarathy et al., 1992; Webster et al., 1998). A weak summer monsoon (as e.g., in 2000) can be accompanied by poor harvests and food shortages and a lack of fresh water among the rural population, which constitutes two thirds of India's total population. On the other hand, a monsoon with higher precipitation than normal (as e.g., in 2005), can cause disastrous floods, again leading to a failure of harvest and food shortage.

Climatologically, the Indian Monsoon is part of a large-scale circulation pattern, known as the Asian Monsoon. The summer monsoon investigated here occurs from June to September and develops due to thermal gradients between the warm Indian continent and the cooler temperatures in the Indian Ocean. The

warmer air masses over land result in areas of low pressure, whereas over the ocean the colder air masses yield higher pressures. This pressure gradient entails the supply of moisture over the Indian continent that ascends, condensates, and is released as precipitation. Several processes influence the Indian monsoon: SSTs of the Indian Ocean (e.g., Clark et al., 2000; Kucharski et al., 2006), land surface characteristics like soil moisture and the surface albedo (e.g., Meehl, 1994; Claussen, 1997; Robock et al., 2003), large scale circulations like the Hadley and the Walker or trade wind circulation (e.g., Webster and Yang, 1992; Krishnamurthy and Goswami, 2000), the orography, e.g., of the Tibetan Plateau (e.g., Liu and Yin, 2002), and the snow cover over Eurasia (e.g., Hahn and Shukla, 1976; Dash et al., 2005).

The influence of anthropogenic activities on the Indian summer monsoon rainfall (ISMR) has been investigated in a number of studies. Most of them indicate that emissions of greenhouse gases, that alter the heat

---

\*Corresponding author: B. KNOPF, knopf@pik-potsdam.de

budget of the system and therefore the land-sea temperature contrast, could increase the monsoon intensity and/or variability (Meehl and Washington, 1993; Zwiers and Kharin, 1998; May, 2002). On the other hand, there is evidence of an aerosol-induced reduction of precipitation (e.g., Patra et al., 2005) or of no clear indication for an influence of global warming at all (Kripalani et al., 2003). In a recent study (Paeth et al., 2008) investigate results of climate model simulations performed in support of the Third Assessment Report of the Intergovernmental Panel on Climate Change (IPCC) (IPCC, 2001) under several greenhouse gas and sulphate aerosol forcing scenarios and find large differences in the projections of the individual models with a probable intensification under enhanced greenhouse conditions. Goswami et al. (2006) show with data analysis that despite a relatively constant mean monsoon precipitation, heavy rainfall events exhibit a rising trend in frequency and magnitude over the last 50 years and Auffhammer et al. (2006) relate air pollution and reduced precipitation caused by climate change to a reduction of rice production in India.

Considering the fact that the impact of climate change on the ISMR is contradictory in different studies and models, the purpose of our study is to understand some of the physical mechanisms that influence the Indian monsoon under climate change and to perform a detailed sensitivity study of the Indian monsoon system. In doing this, we address one of the key questions formulated in the MAIRS initial science plan: “Is the Asian monsoon system resilient to this human transformation of land, water and air?” (MAIRS, 2006).

For our study, we use a box model of the Indian monsoon, which has proven to well reproduce relevant variables, e.g., precipitation averaged over India (Zickfeld, 2004). Because of its transparency, this reduced form model is highly suitable for understanding the effect of anthropogenic perturbations such as emissions of greenhouse gases and sulfur dioxide, and land-cover changes.

This paper is organized as follows: we introduce the box model with the most important equations for the sensitivity study in section 2. The model validation with a profound optimization is given in section 3. In section 4, a detailed sensitivity study with respect to quantities influenced by human action is taken out. Finally, a summary is given in section 5.

## 2. Model setup and data

For our analysis we employ a one-dimensional model of the Indian monsoon that was first presented in Zickfeld et al. (2005) and is described in detail in Zickfeld (2004). It consists of one four-sided box which

is centered over India and is delimited by the Indian Ocean at its eastern, southern and western boundaries and by the Tibetan Plateau at its northern boundary (cf. Fig. 1). In the vertical, the atmosphere is described by three layers: PBL with the surface layer at its lower boundary and the stratosphere as its upper boundary (cf., Fig. 2). The underlying land compartment is represented by two soil layers. The prognostic variables in the model are the near-surface air temperature  $T_a$ , the specific humidity  $q_a$ , and the soil moisture  $w_1, w_2$  of the two soil layers. All other variables such as precipitation, evaporation, net longwave radiation and surface wind are diagnosed from the above-mentioned four. Inside the box, the variables are described in terms of their spatial averages. The only meridional and zonal gradients are those between the box interior (i.e., the Indian sub-continent) and its boundaries, whose climatic conditions (temperature, humidity, cloudiness) are externally prescribed

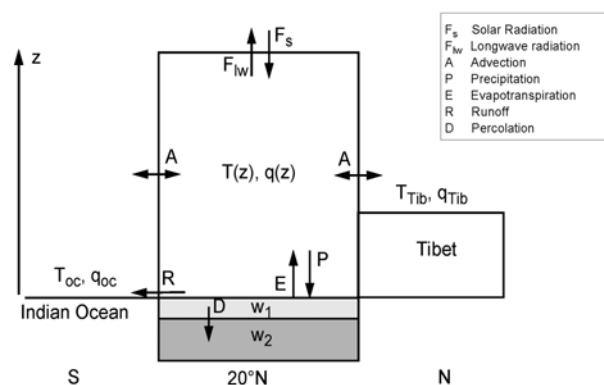


**Fig. 1.** Schematics of the box model of the Indian monsoon.  $T(z), q(z), w_1, w_2$  are calculated prognostically, whereas the climatic conditions at the box boundaries (the temperatures and specific humidities at the oceanic boundaries and over the Tibetan Plateau) are externally prescribed.

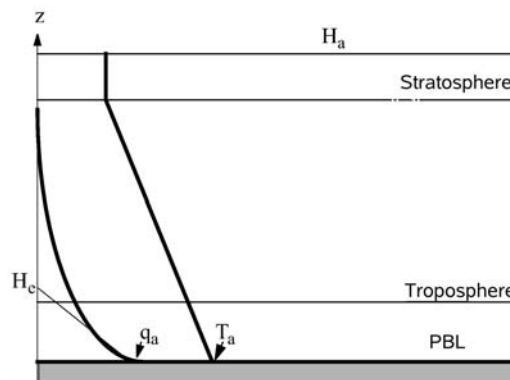


**Fig. 2.** Parameterization of the vertical structure of the atmosphere.

with a seasonal cycle. The associated temperature gradients drive the annual evolution of the local monsoon circulation.

The boundary conditions are prescribed according to the long-term monthly means for 1968–1996 from the NCEP reanalysis data (Kalnay et al., 1996). The northern boundary is defined as the mean over (30°–35°N, 70°–82.5°E), the eastern boundary over (7.5°–17.5°N, 85°–92.5°E), the southern boundary over (0°–5°N, 70°–85°E) and the western boundary over (7.5°–17.5°N, 62.5°–70°E). We prescribe the conditions for surface air temperature  $T_i$ , specific humidity  $q_i$  and cloudiness  $N_i$  at the southern boundary ( $T_S, q_S, N_S$ ), at the western boundary ( $T_W, q_W, N_W$ ), at the eastern boundary ( $T_E, q_E, N_E$ ) and at the northern boundary to the Tibetan Plateau ( $T_{Tib}, q_{Tib}, N_{Tib}$ ). Further, we prescribe the Hadley and the trade wind circulation and the insolation at the top of the atmosphere.

## 2.1 Heat balance

The temporal evolution of the system is computed from the respective balance equations for atmospheric heat and water and soil water content. The heat balance equation for the combined surface-plus-atmosphere system reads:

$$\int_0^{H_a} c_p \rho \frac{\partial \theta}{\partial t} dz + h_s c_s \frac{\partial T_s}{\partial t} = F_{\downarrow} (1 - A_{sys}) - F_{\uparrow} + A_T + \mathcal{L}(C - E), \quad (1)$$

where  $\theta$  is the potential temperature and  $T_s$  the surface temperature.

The first term on the right hand side of Eq. (1) is the incident solar radiation at the top of the atmosphere  $F_{\downarrow}$ , modified by the planetary albedo  $A_{sys}$ . This term is a function of the insolation  $I_0$ , the mean solar zenith angle  $\xi$ , the cloudiness and the albedo of the clouds and the surface. The term  $F_{\uparrow}$ , the net outgoing long-wave radiation at the top of the atmosphere, is treated according to Budyko (1982) as a function of the surface air temperature  $T_a$ , the cloudiness  $N$  over India, and the CO<sub>2</sub> concentration  $p$  in the atmosphere:

$$F_{\uparrow} = A_0 + B_0 (T_a - T_0) - N[C_0 + D_0 (T_a - T_0)], \quad (2)$$

where  $T_0$  is the reference temperature and the coefficients  $A_0, B_0, C_0, D_0$  are functions of the atmospheric CO<sub>2</sub> concentration  $p$  in relation to the reference CO<sub>2</sub> concentration  $p_0$ :

$$X_0 = X_{00} \left[ 1 - \eta \ln \left( \frac{p}{p_0} \right) \right], \quad (3)$$

where  $X \in \{A, B, C, D\}$  and  $X_{00}$  are parameters.

The horizontal advection of heat,  $A_T$ , is described according to Petoukhov et al. (2000) as the vertical integral over the sensible heat flux due to the horizontal circulation and is a sum of the contributions from the local monsoon circulation and the large-scale Hadley and Walker circulations. The surface winds associated with the local monsoon circulation,  $u_{m0,i}$ , are calculated explicitly and computed from the temperature difference between India and the respective boundary:  $u_{m0,i} \sim (T_a - T_i)$ , where  $T_i \in \{T_E, T_S, T_W, T_{Tib}\}$ .

The condensation rate  $C$  is set equal to precipitation, which is also discussed below. The evapotranspiration  $E$  is described in the bulk transfer approach (Hansen et al., 1986). Further,  $H_a$  denotes the height of the atmosphere,  $\rho = \rho(z)$  the air density,  $c_p$  the specific heat of air at constant pressure,  $h_s$  the depth of the upper soil layer and  $c_s$  the heat capacity per unit soil volume which increases along with the water content of the soil.  $\mathcal{L}$  refers to the latent heat of evaporation. In order to reduce the dimensionality of the system, we shall assume  $\partial T_s / \partial t \approx \partial T_a / \partial t$ . This assumption has proven to influence the model behavior only marginally.

## 2.2 Water balance

The vertically integrated water balance equation is given by the expression:

$$\int_0^{H_a} \rho \frac{\partial q}{\partial t} dz = E - C + A_v, \quad (4)$$

where  $q = q(z)$  denotes the vertical profile of specific humidity and  $A_v$  is the horizontal advection of moisture.

The soil moisture, which determines evapotranspiration, is computed prognostically according to a two-layer model Hansen et al. (1986). The rates of change of moisture in the two soil layers are:

$$\frac{\partial w_1}{\partial t} = \frac{P - E - R}{f_1} - \frac{w_1 - w_2}{\tau}, \quad (5)$$

$$\frac{\partial w_2}{\partial t} = \frac{f_1}{f_2} \frac{w_1 - w_2}{\tau}, \quad (6)$$

where the wetness of the  $i$ th layer,  $w_i$ , is the ratio of available water to field capacity  $f_i$  and  $R$  is the surface runoff. The precipitation,  $P$ , is described in accordance with Petoukhov et al. (2000) as:

$$P = \frac{N}{\tau_P} \int_0^{H_t} \rho q dz, \quad (7)$$

where  $N$  is the total cloud amount and  $\tau_P$  the turnover time of water in the atmosphere which is a function of

the vertical velocity,  $w$ :

$$\tau_P = \tau_0 \left\{ 1 - a_\tau 0.5 \left[ 1 + \tanh \left( \frac{w}{a_3} \right) \right] \right\}. \quad (8)$$

$\tau_0$ ,  $a_\tau$  and  $a_3$  are parameters.

The vertical velocity  $w$  at the upper boundary of the PBL is derived from the continuity equation as the sum of the contributions due to the monsoon and the Hadley circulations.

The surface runoff  $R$  is assumed to be proportional to precipitation and water content of the upper soil layer Hansen et al. (1986).  $\tau$  denotes the time constant for diffusion of moisture between the two layers.

### 2.3 Vertical structure of the atmosphere

The vertical profile of the temperature,  $T(z)$ , is parameterized in terms of the near surface value  $T_a$  with a linear profile in the troposphere ( $T(z) = T_a - \Gamma z$ ) and a constant profile in the stratosphere ( $T(z) = T_a - \Gamma H_t$ ), cf., Fig. 2. The lapse rate  $\Gamma$  is described according to Petoukhov et al. (2003):

$$\Gamma = \Gamma_0 + \Gamma_1 (T_a - T_0) (1 - a_q q_a^2) - \Gamma_2 N_{cu}, \quad (9)$$

with parameters  $\Gamma_0, \Gamma_1, \Gamma_2, a_q$  and  $N_{cu}$  the cumulus cloud amount. The specific humidity  $q(z)$  is assumed to decrease exponentially with height:

$$q(z) = q_a \exp \left( -\frac{z}{H_e} \right), \quad (10)$$

where  $H_e$  is the water vapor scale height.

$$V = \begin{cases} 0 & \text{if } P < P_{cr} \\ 1 - \frac{1}{1 + a_v (P - P_{cr})^2} & \text{otherwise (for } V < V_{max}, \text{ else } V = V_{max}) \end{cases}, \quad (13)$$

where  $P_{cr}$  is a threshold value of annual mean precipitation below which the vegetation cover cannot be sustained in the long term.  $V_{max}$  is the maximal possible vegetation cover and  $a_v$  is a parameter.

## 3. Model validation

The model described above includes a number of parameters, some of which are physical constants or known from observations. However, most parameters are to some degree model dependent (“tunable”). To choose these parameter values adequately, we first perform a 2-step procedure to determine the parameter settings that best fit the observational data. As the variable of interest, we use the deviation from the ob-

## 2.4 Land surface parameterization

The albedo of the land surface,  $A_s$ , influences the heat budget of the system through the planetary albedo,  $A_{sys}$ . It is computed as the weighted sum of the albedos of vegetated and bare soil,  $A_{sv}$  and  $A_{sb}$ , respectively:

$$A_s = V A_{sv} + (1 - V) A_{sb}, \quad (11)$$

where  $V$  is the fraction of the land surface covered by vegetation. The albedo of the vegetated soil is determined by the type of vegetation cover. The bare soil albedo is dependent on the soil color (which is prescribed) and the water content of the upper soil layer Dickinson et al. (1986).

The surface roughness  $z_0$  is used to calculate the cross-isobar angle which determines the local monsoon circulation,  $u_{m0,i}$ , and the drag coefficients for the fluxes of water and heat. In the model,  $z_0$  is a combination of the roughness of the surface covered by vegetation,  $z_v$ , and the roughness of the bare soil,  $z_b$ . It is computed by combining the drag coefficients for bare and vegetated soil (Claussen, 1991):

$$\left( \ln^2 \frac{z_s}{z_0} \right)^{-1} = V \left( \ln^2 \frac{z_s}{z_v} \right)^{-1} + (1 - V) \left( \ln^2 \frac{z_s}{z_b} \right)^{-1}, \quad (12)$$

where  $z_s$  is the blending height.

$V$  is calculated according to Brovkin et al. (1998) as a hyperbolic function of precipitation  $P$ :

served seasonal cycle of precipitation over India (Eq. 14). The first step consists of identifying those parameters that have the strongest influence on the seasonal cycle of precipitation. Subsequently, these parameters are optimized so as to minimize the cost function.

### 3.1 Global sensitivity analysis

The scope of the global sensitivity analysis (GSA) is to identify those parameters that have the largest (the smallest) effect on the seasonal cycle of precipitation and to come up with a ranking of the parameters according to their importance. We choose 46 model parameters<sup>a</sup> (this set will in the following be referred to as  $S_{46}$ .) with the uncertainty ranges indicated in Table 1. We calculate the influence of these param-

<sup>a</sup>The other parameters are physical constants.

**Table 1.** Results of the global sensitivity analysis and the optimization. Listed are the ten most influential parameters of the parameter set  $S_{46}$  in order of decreasing importance, along with the ranges used in the global sensitivity analysis and the optimization, the mean distance  $\mu$  (see text for definition), and the optimal value.

Parameter	Range	$\mu$	Optimal value	Units
$\tau_0$	$(2.5-6) \times 10^5$	2.13	$5.41 \times 10^5$	s
$z_v$	0.01–0.8	1.25	0.06	m
$G_k$	0.1–0.8	1.09	0.78	L
$a_q$	700–4000	0.93	734.1	$\text{kg}^2 \text{kg}^{-2}$
$z_s$	10–100	0.70	36.08	m
$a_1$	0.64–0.96	0.56	0.64	L
$G_{h,1}$	2–6	0.48	5.99	L
$\tau_{st}$	5–15	0.44	14.80	L
$G_{k,1}$	8–20	0.39	8.94	L
$B_{00}$	1.6–2.3	0.39	2.27	$\text{W m}^{-2} \text{K}^{-1}$

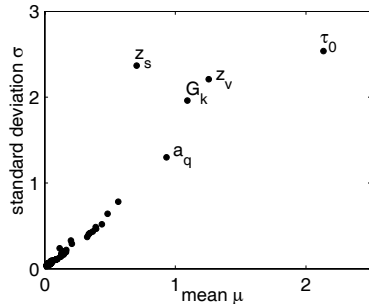


**Fig. 3.** Results of the global sensitivity analysis. The mean distance  $\mu$  is a measure of the influence of a parameter on the cost function  $F$  (Eq. 14), with higher values meaning stronger influence. A high variance  $\sigma$  indicates that the effect of a parameter on the cost function  $F$  is non-linear. The most influential parameters are labeled.

ters on the deviation of the seasonal cycle of modeled precipitation  $P_{\text{mod}}$  from the long-term mean observed value  $P_{\text{obs}}$ :

$$F = \sum_{i=1}^{12} |P_{\text{mod},i} - P_{\text{obs},i}|, \quad (14)$$

where  $P_{\text{mod},i}$ ,  $P_{\text{obs},i}$  ( $i = \text{January}, \dots, \text{December}$ ) are monthly-mean values. As reference values,  $P_{\text{obs}}$ , we use the All India Rainfall (AIR) index (Parthasarathy et al., 1995). Eq. (14) will also be used as cost function for the parameter optimization.

To identify the most influential parameters we apply the multi-run simulation environment SimEnv (Flechsigt et al., 2005; SimEnv, 2006). The method applied by SimEnv is the Morris method (Morris, 1991), modified by Campolongo et al. (2005). The uncertainty ranges of the 46 parameters are subdivided into equal  $m = 8$  intervals for each parameter.

On the resulting regular grid of  $(m + 1)^{46}$  grid points the Morris method lays random trajectories

through this 46-dimensional space, whereby two adjacent points on a trajectory only differ in one parameter  $s_i$ . The points are simultaneously adjacent grid points and each  $s_i$  is varied only once on every trajectory. In the parameter space this results in trajectories with 46+1 points. Measured is the distance  $\Delta F_{ij}$  between the two values for the variable  $F$  of the  $j$ th trajectory with respect to the parameter  $s_i$  that is varied. Two statistical measures are derived for each parameter  $s_i$  from this analysis: the mean absolute value  $\mu_i = \text{mean}(|\Delta F_i|)$  and the standard deviation  $\sigma_i = \sigma(\Delta F_i)$  over all trajectories. A high mean value,  $\mu_i$ , is interpreted as an important overall influence of the parameter on the model output  $F$ . A high variance  $\sigma_i$  indicates that the parameter is involved in interactions with other parameters with respect to the model output or that the effect of the parameter on the model output is non-linear (Saltelli et al., 2004).

Here, we randomly sample 300 trajectories, resulting in  $(46+1) \times 300 = 14100$  sample points and single model runs in total. Although these runs only cover a small part of the whole parameter space, the ranking is found to be robust.

The ranking according to the value of  $\mu$  deduced from this analysis is given in Table 1. We obtain a clustering of the parameters with only a few highly influential parameters and a majority of parameters with low influence. We find that the most influential parameters are those that determine either precipitation directly (such as the characteristic precipitation time  $\tau_0$ , cf. Eq. (8) or the monsoon circulation  $u_{m,i}(z)$  (via the parameters  $G_k, G_{h,1}, G_{k,1}$  that determine the cross-isobar angle) and therefore the advection of heat,  $A_T$ , and moisture,  $A_v$ .

### 3.2 Optimization and validation

With the identification of the most influential parameters, we hold in hand the prerequisite to optimize

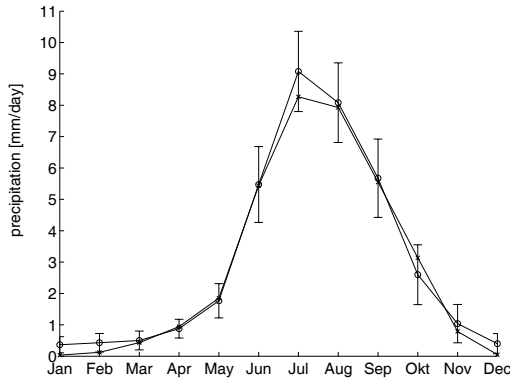


**Fig. 4.** Comparison of the monthly values for the seasonal cycle of precipitation for observational data (open circles) and the optimized model (crosses). The vertical bars encompass two standard deviations. Observational data are taken from Parthasarathy et al. (1995).

the model efficiently. We choose the ten most influential parameters for the optimization procedure. The optimization is performed with SimEnv with an Adaptive Simulated Annealing (Ingber, 1996) procedure to allow for finding the global minimum of the cost function. As a cost function we choose the deviation from the observed annual cycle of precipitation, as given by Eq. (14).

The optimal parameter settings are listed in Table 1. With this setting the model reproduces the observed annual cycle of monsoon precipitation very well (cf., Fig. 4). The deviance from the long term summer monsoon rainfall for June–September (JJAS) of 849 mm is 2%. Moreover, onset and offset of the summer monsoon are captured correctly by our model.

Qualitatively, the annual cycle of the monsoon as simulated by our box model closely resembles the observed monsoon dynamics for the surface temperature,  $T_a$ , and the specific humidity,  $q_a$ , (cf., Fig. 5). For the soil moistures,  $w_1$  and  $w_2$ , it is hardly possible to show corresponding observational data. The correspondence between model results and data is also satisfactory in quantitative terms, except that the temperature over India is modelled as too high with no significant cooling in winter. As a consequence, the land is slightly warmer than the surrounding ocean, even in winter, such that the land-ocean temperature gradient is not truly reversed. This is caused by the fact that with our model we can only represent the local monsoon circulation and not the large-scale circulation, e.g., the Hadley circulation, which is only included as a boundary condition. Moreover the model does not account for the influence of the Tibetan Anticyclone and Transverse Monsoon, which are specifically important in winter.

All in all, our simple model performs well in simu-

lating the observed monsoon dynamics. This demonstrates that despite its high degree of idealization the model captures the essential physical processes and feedback mechanisms.

#### 4. Sensitivity analysis

In this section, we describe the sensitivity of Indian rainfall to variations of the model parameters and boundary conditions. We devote particular attention to the quantities influenced by human actions. Three different kinds of anthropogenic forcing are considered here: (i) emissions of greenhouse gases (GHGs), (ii) emissions of aerosol-generating substances (mainly  $\text{SO}_2$ ) and (iii) land-cover changes. GHG emissions lead to higher  $\text{CO}_2$  concentrations and different climate conditions at the boundaries (e.g., higher boundary temperatures  $T_i$ ).  $\text{SO}_2$  emissions result in higher particle concentrations in the atmosphere, which affects the back-scattering of solar radiation, the radiative properties of clouds, and the cloud droplet size and hence the precipitation efficiency. We take the latter two effects into account by increasing the optical thickness of stratus clouds,  $\tau_{\text{st}}$ , which in turn increases the planetary albedo,  $A_{\text{sys}}$ , and by increasing the characteristic precipitation time,  $\tau_0$  (Eq. 8), which leads to a reduction in precipitation. Land-cover changes such as forest conversion or desertification cause a decrease of the roughness length of vegetated soil  $z_v$  (Eq. 12) on one hand and an increase in the albedo of vegetated soil,  $A_{\text{sv}}$ , on the other (Eq. 11). Desertification is taken into account in our model by decreasing the maximum fractional vegetation cover,  $V_{\text{max}}$  (Eq. 13).

In the following, we first investigate the sensitivity of Indian rainfall to changes in single parameters (section 4.1). We then perform a combined sensitivity analysis, whereby we group the parameters that can be affected by a specific human intervention (e.g.,  $p$  and  $T_i$ , which are both influenced by anthropogenic GHG emissions) (section 4.2). Finally, we choose the most influential parameter out of the three groups (i)–(iii) of potential human actions and investigate the sensitivity of Indian rainfall to simultaneous changes in those parameters (section 4.3).

##### 4.1 Sensitivity of single parameters

The parameters varied in the course of the sensitivity analysis are listed in Table 2 along with the values employed. The annual cycle of precipitation for each parameter is given in Fig. 6. Table 2 summarizes the Indian summer (JJAS) precipitation and the onset/offset of the summer monsoon for each experiment. Summer monsoon onset is defined as the time when precipitation begins to rise sharply, which corresponds to a switch in the vertical velocity from negative to

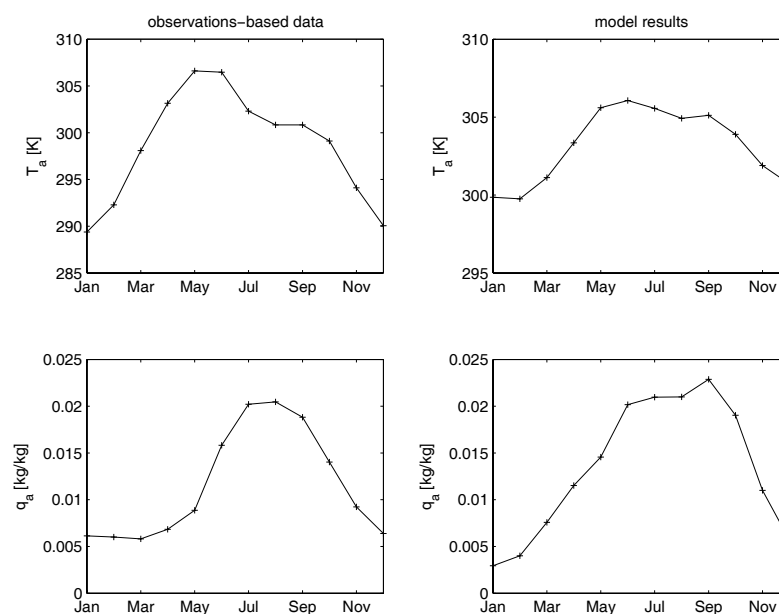


**Fig. 5.** Seasonal cycle of the surface temperature,  $T_a$ , and the specific humidity,  $q_a$ , for observations-based data (left column) and as simulated by the optimized model (right column). For the observations-based data monthly long term mean values from the NCEP/NCAR reanalysis project (Kalnay et al., 1996) are averaged over ( $15^\circ\text{N}$ – $25^\circ\text{N}$ ,  $75^\circ\text{E}$ – $80^\circ\text{E}$ ).

**Table 2.** Summer monsoon precipitation (JJAS) and onset/offset for different choices of anthropogenically influenced parameters. The standard model values are given in bold.

Parameter	Value	Units	Precipitation (mm)	Anomaly (%)	Onset/offset (month)
$\tau_0$	$2.5 \times 10^5$	s	1437	65.5	3.8/8.8
	$5 \times 10^5$	s	917	5.7	4.3/8.6
	<b><math>5.4 \times 10^5</math></b>	s	868	0	4.3/8.6
	$7.5 \times 10^5$	s	673	-22.5	4.5/8.5
$z_v$	0.01	m	773	-10.9	4.5/8.6
	<b>0.06</b>	m	868	0	4.3/8.6
	0.1	m	897	3.3	4.2/8.6
	0.3	m	927	6.8	4.0/8.5
$\tau_{st}$	5	L	954	9.9	4.1/8.9
	10	L	907	4.5	4.2/8.7
	<b>14.8</b>	L	868	0	4.3/8.6
	15	L	866	-0.1	4.3/8.6
$A_{sv}$	0.1	L	924	6.4	4.2/8.7
	<b>0.16</b>	L	868	0	4.3/8.6
	0.2	L	834	-3.9	4.4/8.5
	0.3	L	725	-16.5	4.7/8.2
$p$	280	ppm	857	-1.2	4.3/8.5
	<b>360</b>	ppm	868	0	4.3/8.6
	560	ppm	885	2	4.3/8.5
	1120	ppm	913	5.2	4.3/8.5
$V_{max}$	0.5	L	586	-32.4	4.4/8.5
	0.75	L	744	-14.2	4.3/8.6
$\Delta T_{oc}$	<b>1</b>	L	868	0	4.3/8.6
	-1	K	825	-4.9	4.4/8.6
	<b>0</b>	K	868	0	4.3/8.6
	2.5	K	963	11	4.2/8.5
	5	K	1042	20.1	3.8/8.4

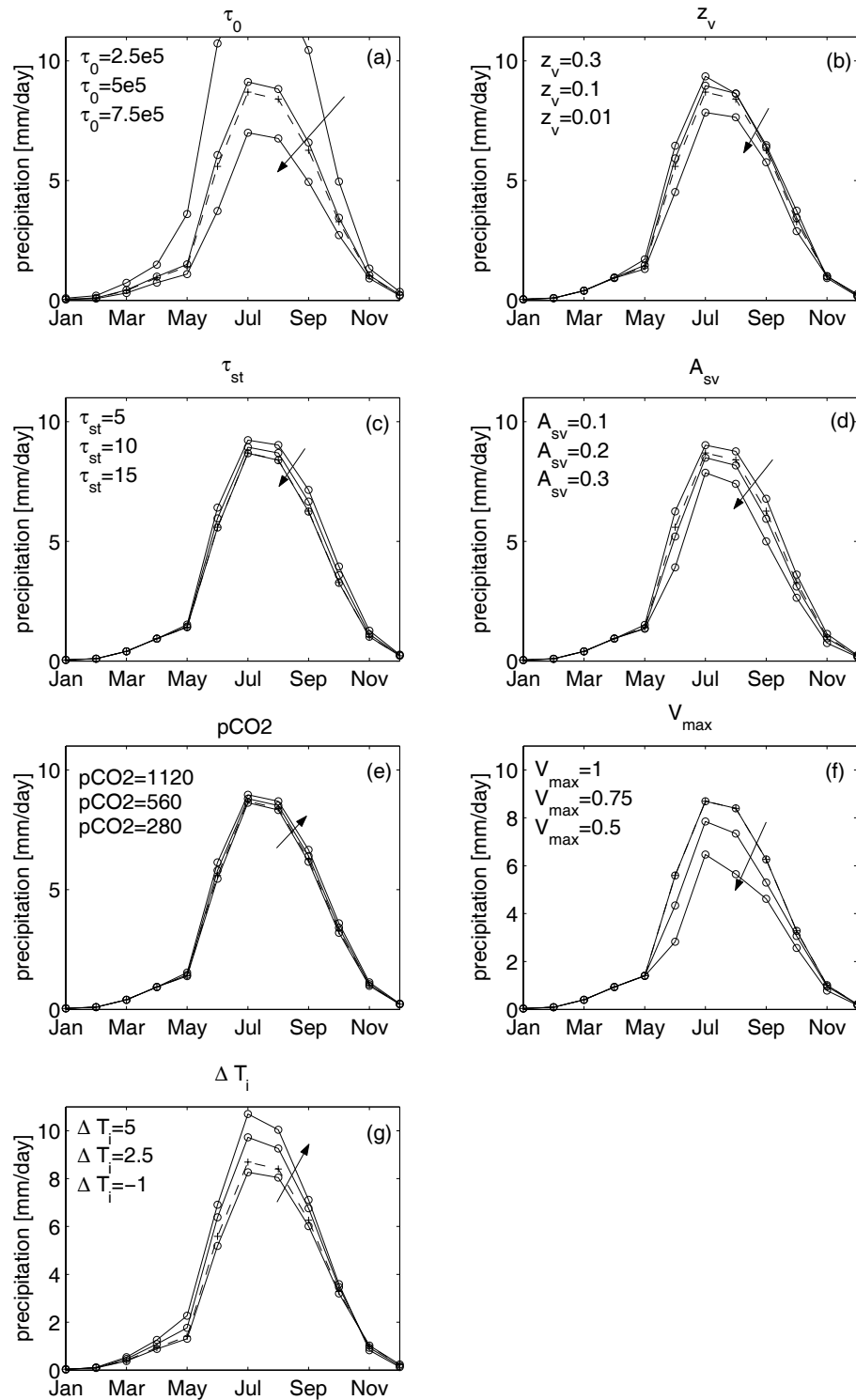


**Fig. 6.** Sensitivity of monthly mean precipitation to: (a)  $\tau_0$  (units: s), (b)  $z_v$  m, (c)  $\tau_{st}$  (units: L), (d)  $A_{sv}$  (units: L), (e)  $p$  (units: ppm), (f)  $V_{max}$  (units: L) and (g)  $\Delta T_i$  (units: K). The solid lines are associated with the given parameter values (from top to bottom). The dashed line is the result of the standard model. The arrows indicate the direction of change related to anthropogenic perturbations.

positive values and the startup of cumulus convection. The monsoon withdrawal is defined as the time the vertical velocity again switches to negative values.

Figure 6 indicates that the variation of most of the anthropogenically influenced parameters mainly affects the summer precipitation over India. The magnitude and direction of summer precipitation changes differ among parameters. Increases in the  $\text{CO}_2$  concentration,  $p$ , to two and four times the pre-industrial value lead to only a slight increase in summer precipitation relative to the present-day (2% to 5%). More significant changes in precipitation are modeled for a temperature increase at the four boundaries,  $\Delta T_i$  with  $i \in \{\text{E, S, W, Tib}\}$ , of 2.5 K and 5 K (11% and 20%). Increases in both the optical thickness of stratus clouds,  $\tau_{\text{st}}$ , and the surface albedo,  $A_{\text{sv}}$ , relative to the standard values result in a decrease in summer rainfall. The reason is higher planetary albedo, reduced solar radiation penetrating to the surface, a weakening of land-to-ocean temperature contrast and hence, the monsoon circulation. A longer characteristic precipitation time,  $\tau_0$ , expectedly leads to a decrease in precipitation. The changes in summer precipitation are large, amounting to a decrease by 22.5% for the high  $\tau_0$  value. A decrease in the surface roughness also leads to reduced precipitation. The mechanism through which this occurs is a decrease in the cross-isobar angle and hence, the monsoon circulation. A decrease in  $V_{\text{max}}$  acts to reduce rainfall through two mechanisms: the increase in surface albedo,  $A_{\text{sv}}$ , and the decrease in surface roughness,  $z_0$ , (albedo is higher for bare than for vegetated soil and surface roughness is lower), which both weaken the monsoon circulation.

Overall, the influence of parameter changes on the summer monsoon precipitation (JJAS) is large, with changes ranging from +65% to -32.4%. By far the largest influence is the turnover time of water in the atmosphere  $\tau_0$ . The value for  $\tau_0$  that results from the tuning is 6.25 days, which is well in line with the value of 3–10 days discussed in literature. Fixing all other parameters to their standard values, the observed variability of precipitation can be represented by a range for  $\tau_0$  between  $4.6 \times 10^5$  and  $6.3 \times 10^5$  (i.e., between 5.3 and 7.3 days). This indicates the realism of this model for the Indian monsoon precipitation.

The direction of precipitation change is opposite among the different types of human actions considered: whereas summer monsoon precipitation decreases for changes in all parameters associated with higher aerosol emissions, conversion of forest cover and desertification, precipitation increases under anthropogenic  $\text{CO}_2$  emissions. This indicates that, ultimately, the sign of precipitation changes over India will depend on the direction and relative magnitude

of the different human interventions. To gain insight in the coeval dependence of Indian rainfall on the different forcings, a combined parameter study is carried out (section 4.3).

Changes in summer monsoon on- and offset are small for most parameter variations. Significant changes occur only for the characteristic precipitation time,  $\tau_0$ , and the boundary temperature anomalies,  $\Delta T_i$ . The duration of the summer monsoon season is shortened by 9 days for  $\tau_0 = 7.5 \times 10^5$  s and lengthened by 9 days for  $\Delta T_i = 5$  K.

For the investigated parameter ranges, the model responds, in most cases, linearly to the parameter changes, except for  $\tau_0$  and  $A_{\text{sv}}$ . In an earlier study (Zickfeld et al., 2005) we showed that a reduced form of the monsoon model exhibits a saddle node bifurcation with a regime shift from a wet to a dry monsoon regime in dependence of those parameters that influence the heat budget of the system. This strongly nonlinear decrease in precipitation is also seen in this model, for instance in dependence of the surface albedo,  $A_{\text{sv}}$ . The “critical” value of for  $A_{\text{sv}}$  of approximately 0.45, however, is beyond the plausible range for  $A_{\text{sv}}$ .

#### 4.2 Sensitivity to elevated $\text{CO}_2$ and $\text{SO}_4$ concentrations

In the above experiments the parameters were varied ad hoc. In order to gain a quantitative understanding of ISMR responses under plausible scenarios of global change, we perform a set of experiments with changes in parameters that can be related to a doubling and quadrupling of the pre-industrial  $\text{CO}_2$  concentration. We also perform an experiment with increased atmospheric sulfate burden.

Given that the conditions at the box boundaries have to be prescribed externally, the choice of the specific climate change scenario is limited to the already existing simulations with coupled climate models of global scale. Here we use the CLIMBER-2 model as reference and take the anomalies in the boundary conditions from an equilibrium  $2 \times \text{CO}_2$  experiment with this model (Ganopolski et al., 2001). We further consider scenarios with  $\text{CO}_2$  concentrations increased to four times the pre-industrial value by linear extrapolation of the boundary conditions for the  $2 \times \text{CO}_2$  case (cf., Table 3). This is only a crude approximation since the response of the climate system to large concentration changes is certainly not linear, but given the overall simplicity of the model and the exploratory purpose of these experiments, we think it is a valid assumption.

We calculate the equilibrium response of the annual cycle of the Indian monsoon to the two  $\text{CO}_2$  forcings. Our results indicate a strengthening of the hydrological cycle under increased  $\text{CO}_2$  conditions. In the

**Table 3.** Anomalies in the boundary conditions and parameters imposed in the experiments with increased CO<sub>2</sub> and sulfate aerosol concentrations.  $\Delta u_{tr,max}$  describes the trade wind anomalies,  $\Delta v_{H,0}$  the anomalies of the Hadley circulation,  $B_{SO_4}$  is the total column concentration of SO<sub>4</sub>.

Parameter (units)	2×CO <sub>2</sub>		4×CO <sub>2</sub>		SO <sub>4</sub>	
	Summer	Winter	Summer	Winter	Summer	Winter
$\Delta T_{S,E,W}$ (K)	2.5	2.5	5	5	-	-
$\Delta T_N$ (K)	3	4	6	8	-	-
$\Delta u_{tr,max}$ (m s <sup>-1</sup> )	-0.25	-0.25	-0.5	-0.5	-	-
$\Delta v_{H,0}$ (m s <sup>-1</sup> )	-0.02	0.02	-0.04	0.04	-	-
$p$ (ppm)	560	560	1120	1120	360	360
$B_{SO_4}$ (mg m <sup>-2</sup> )	-	-	-	-	25	25
$\tau_{st}$ (L)	-	-	-	-	18	18
$\tau_0$ (s)	-	-	-	-	$6.5 \times 10^5$	$6.5 \times 10^5$

**Table 4.** Summer monsoon precipitation (JJAS) and onset/offset for the experiments with increased CO<sub>2</sub> and sulfate aerosol concentrations in relation to the reference model (CTL).

Experiment	JJAS precipitation (mm)	Anomaly (%)	Onset/offset (month)
2×CO <sub>2</sub>	961	10.7	4.1/8.5
4×CO <sub>2</sub>	1060	22.1	3.8/8.5
SO <sub>4</sub>	667	-23.0	4.6/8.2
CTL	868	0	4.3/8.6

2×CO<sub>2</sub> and 4×CO<sub>2</sub> experiments JJAS precipitation over India increases by nearly 11% and 22%, respectively (cf., also Fig. 7 and Table 4). This increase in precipitation is well in line with studies analysing projections of state-of-the-art GCMs, e.g., those used in support of the Fourth Assessment Report (AR4) of the Intergovernmental Panel on Climate Change (IPCC): Annamalai et al. (2007), e.g., report an increase in mean monsoon rainfall of 5%–25% over the Indian subcontinent for CO<sub>2</sub> doubling, Kripalani et al. (2007) report an increase in mean monsoon precipitation of 8% for the south Asian region.

In our model, this observed strengthening of the hydrological cycle is due to higher specific humidity over the oceans which leads to stronger landward advection of moisture and hence increased convection, cumulus cloudiness and precipitation.

Perhaps surprisingly, the temperature contrast between the Indian Ocean and the Indian peninsula is reduced slightly under increased CO<sub>2</sub> conditions (since  $T_a$  increases less than  $T_S$ ,  $T_E$  and  $T_W$ ). As a consequence, the monsoon circulation weakens relative to the present-day strength. There are two explanations for this behavior. The reduction in the temperature contrast could be due to different sensitivities to CO<sub>2</sub> concentrations of the radiative scheme implemented in the CLIMBER-2 model, which is used to determine

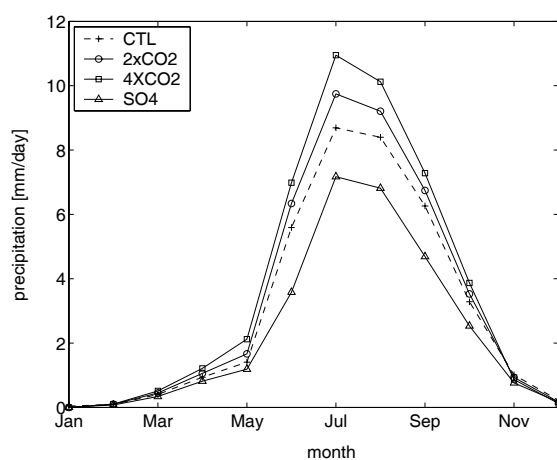


**Fig. 7.** Annual cycle of monthly mean Indian rainfall for the reference model (CTL) and the experiments with increased CO<sub>2</sub> and sulfate aerosol concentrations (2×CO<sub>2</sub>, 4×CO<sub>2</sub>, SO<sub>4</sub>).

the temperatures at the boundaries, and the Budyko (1982) scheme used in the present model. Alternatively, the weakening of the temperature gradient may be associated with increased cumulus cloud cover which reduces the amount of solar radiation penetrating to the surface. This explanation is consistent with GHG experiments with comprehensive models which indicate a local minimum of temperature increase over India due to significant changes in the hydrological cycle (Kitoh et al., 1997).

In a subsequent experiment, we investigate the response of the Indian monsoon to increased anthropogenic sulfur emissions. Given that our model does not include a proper representation of the sulfur chemistry, the aerosol forcing is treated in a highly idealized way. The direct radiative effect due to back-scattering of solar radiation in the clear-sky atmosphere is expressed as a perturbation of the surface albedo depending on the total sulfate aerosol burden in the atmospheric column (Mitchell et al., 1995; Meehl et al.,

1996; Haywood, 1997):

$$\Delta A_s = (1 - A_s)^2 k_e B_{\text{SO}_4} \beta \cos(\xi)^{-1}, \quad (15)$$

where  $k_e$  is the specific extinction coefficient of sulfate aerosol,  $B_{\text{SO}_4}$  is the total column burden of sulfate and  $\beta$  is the backscattered fraction.  $k_e$  and  $\beta$  are set to values of  $8 \text{ m}^2 \text{ g}^{-1}$  and 0.29 (Mitchell et al., 1995). The sulfate aerosol concentration is taken from a study in which a chemical transport model coupled to an AOGCM is driven by IPCC emission scenario IS92a (Roeckner et al., 1999). The employed value of  $25 \text{ mg m}^{-2}$  corresponds to the decadal mean for 2040–2050 over India. For a surface albedo of 0.16 (which corresponds to the summer value in our model), the above formula leads to an increase in surface albedo by almost 50%.

The first indirect aerosol effect is taken into account by increasing the optical depth of stratus clouds,  $\tau_{\text{st}}$ , by 20%. This increment is the result of educated guesswork rather than a value derived from model simulations. The procedure, however, to consider the indirect aerosol effect via increase in cloud albedo is applied in studies with complex models as well (cf., e.g., Meehl et al., 1996). Through their effects on the size of cloud droplets, aerosols also affect precipitation directly. In fact, large concentrations of aerosols nucleate smaller droplets that coalesce inefficiently into raindrops (Rosenfeld, 2000). We account for this effect by increasing the characteristic precipitation time,  $\tau_0$ , by 20%.

The parameter settings used in the aerosol experiment (denoted “SO<sub>4</sub>”) are summarized in Table 3. Note that we leave the conditions at the boundaries unchanged given that the aerosol loading is found to be mainly concentrated over the Asian continent (Roeckner et al., 1999).

Our results indicate that the increased reflectivity of the atmosphere under both clear-sky and cloudy conditions leads to a reduced fraction of solar energy entering the systems. This leads to a weakening of the land-ocean temperature contrast and, in turn, the monsoon circulation. As a consequence, landward advection of moisture, evaporation and precipitation are reduced. This general weakening of the hydrological cycle is amplified by the direct effect of the aerosols on precipitation. In fact, higher  $\tau_0$  decreases the precipitation efficiency [defined here as  $1/\tau_P$ ; cf., Eq. (7)], and, in turn, the latent heat release to the atmosphere. This further weakens the land-sea temperature contrast. The overall effect of the scattering aerosols is a reduction of summer precipitation by as much as 23% (cf., Fig. 7 and Table 4).

### 4.3 Combined sensitivity analysis

So far, we have analyzed the effects of changes in

parameters related to each type of human interaction separately. In order to get a sense of which effect will ultimately dominate, we take the most influential parameter out of every subset (i)–(iii) described in section 4.2, i.e., (i) GHG emissions, (ii) sulfur dioxide emissions, and (iii) land-cover changes. These are (i) the temperature anomalies at the boundaries  $\Delta T_i$ , (ii) the turnover time of precipitation  $\tau_0$ , and (iii) the maximal vegetation cover  $V_{\text{max}}$ . We use three values for each parameter (cf., Table 2), which results in a  $3^3$  dimensional grid, and explore the sensitivity of ISMR to these parameter changes (cf., Fig. 8).

From Fig. 8 it can be deduced that it strongly depends on the exact value the three analyzed parameters will take in the future whether human activities will lead to a decrease or increase of monsoon precipitation. The range of possible responses ranges from a decrease by 52% to an increase by 115%.

Both of these changes would likely challenge the adaptive capacity of the rural population in India. As a worst-case scenario, a “roller-coaster” effect is possible (Zickfeld et al., 2005), whereby the monsoon precipitation first decreases strongly due to increasing aerosol concentrations, but then suddenly increases as the effect of increased CO<sub>2</sub> concentration and rising ocean temperatures become manifest.

## 5. Summary and conclusions

In this paper, we presented an in-depth analysis of the sensitivity of Indian summer monsoon rainfall to changes in parameters and boundary conditions which are influenced by human activities. The analysis was conducted using a one-dimensional box model of the tropical atmosphere centered over India, which includes parameterizations of the radiative and surface

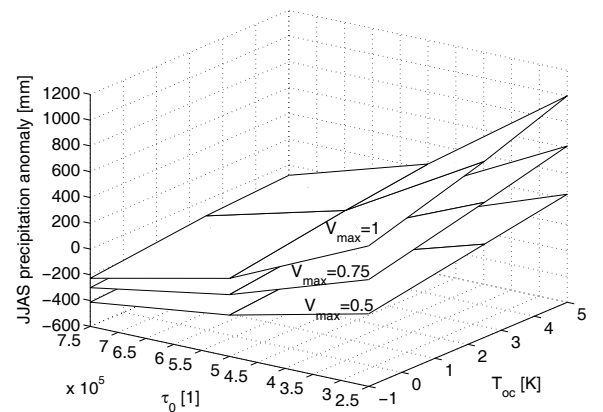


**Fig. 8.** Results of the combined sensitivity analysis. Shown is the summer (JJAS) monsoon precipitation anomaly with respect to the standard model value of 868 mm.

fluxes, the hydrological cycle and surface hydrology. Despite its simplicity, the model can be optimized so as to satisfactorily reproduce key features of the observed monsoon dynamics such as the annual course of precipitation and the transitions between winter and summer regimes. The advantages of this model are its computational efficiency, which allows one to perform a large number of sensitivity experiments, and its transparency, which allows for a clear understanding of the physical mechanisms behind the model response.

We first performed a set of sensitivity experiments, whereby nine model parameters were varied independently. These parameters can be associated with human emissions of greenhouse gases, emissions of aerosols and land-cover changes. We find that changes in those parameters which are related to emissions of greenhouse gases ( $\text{CO}_2$  concentration and surface air temperature at the boundaries) lead to an increase in Indian summer rainfall. In contrast, all parameters related to higher atmospheric aerosol concentrations (the planetary albedo and the characteristic precipitation time) lead to a decrease in Indian rainfall. Similarly, changes in parameters which can be related to forest conversion or desertification (the surface albedo and roughness), act to decrease the summer precipitation.

In the above experiments the parameters were varied ad hoc. In order to gain a quantitative understanding of ISMR responses under plausible scenarios of global change, we perform a set of climate change experiments, with changes in parameters that can be related to a doubling and quadrupling of the pre-industrial  $\text{CO}_2$  concentration. We also perform an experiment with an increased atmospheric  $\text{SO}_4$  burden. Results of a set of GHG experiments indicate that under  $2\times\text{CO}_2$  and  $4\times\text{CO}_2$  conditions, summer precipitation over India increases. This occurs despite a slight weakening of the land-ocean temperature contrast and hence, a slackening of the monsoon circulation. The reason for this is higher humidity over the oceans which leads to increased landward advection of moisture. Results of an aerosol experiment indicate that under enhanced atmospheric sulfate loading alone, summer precipitation is reduced considerably. The reason is the cooling of the Indian subcontinent relative to the adjacent oceans.

Which direction of change will ultimately prevail under plausible scenarios of human intervention? To answer this question we have chosen the most influential parameter for each type of human intervention (the temperature at the oceanic boundaries, the maximum vegetation cover and the characteristic precipitation time). Our results indicate that the sign of precipitation changes over India will depend on the

direction and relative magnitude of human perturbations. A likely scenario is that emissions of greenhouse gases will increase atmospheric  $\text{CO}_2$  concentrations to at least twice the pre-industrial values and that because of their adverse effects on human health and food production  $\text{SO}_2$  emissions will start to decline. Under such assumptions, our model projects ISMR to increase. Large changes in vegetation cover towards deserts, however, have the potential to offset some of this change.

**Acknowledgements.** Part of this work was funded by the German Research Association (DFG) (PR1175/1-1).

## REFERENCES

- Annamalai, H., K. Hamilton, and K. R. Sperber, 2007: The South Asian Summer Monsoon and its relationship with ENSO in the IPCC AR4 simulations. *J. Climate*, **20**(6), 1071–1092.
- Auffhammer, M., V. Ramanathan, and J. R. Vincent, 2006: Integrated model shows that atmospheric brown clouds and greenhouse gases have reduced rice harvests in India. *PNAS*, **103**(52), 19668–19672.
- Brovkin, V., M. Claussen, V. Petoukhov, and A. Ganopolski, 1998: On the stability of the atmosphere-vegetation system in the Sahara/Sahel region. *J. Geophys. Res.*, **103**(D24), 31613–31624.
- Budyko, M., 1982: *The Earth's Climate*. Vol. 29, *International Geophysics Series*. Academic Press, New York, 307pp.
- Campolongo, F., J. Cariboni, A. Saltelli, and W. Schoutens, 2005: Enhancing the Morris Method. *Sensitivity Analysis of Model Output. Proceedings of the 4th International Conference on Sensitivity Analysis of Model Output (SAMO 2004)*, Los Alamos National Laboratory, Los Alamos. 369–379.
- Clark, C. O., J. E. Cole, and P. J. Webster, 2000: Indian Ocean SST and Indian summer rainfall: Predictive relationships and their decadal variability. *J. Climate*, **13**(14), 2503–2519.
- Claussen, M., 1991: Estimation of areally-averaged surface fluxes. *Bound.-Layer Meteor.*, **54**, 387–410.
- Claussen, M., 1997: Modeling bio-geophysical feedback in the African and Indian monsoon region. *Climate Dyn.*, **13**(4), 247–257.
- Dash, S. K., G. P. Singh, M. S. Shekhar, and A. D. Vernekar, 2005: Response of the Indian summer monsoon circulation and rainfall to seasonal snow depth anomaly over Eurasia. *Climate Dyn.*, **24**, 1–10.
- Dickinson, R., A. Henderson-Sellers, P. Kennedy, and M. Wilson, 1986: Biosphere-atmosphere transfer scheme (bats) for the NCAR community climate model. Technical report, National Center for Atmospheric Research, Boulder, US, 69pp.
- Flechsig, M., U. Böhm, T. Nocke, and C. Rachimow,

- 2005: Techniques for quality assurance of models in a multi-run simulation environment. *Sensitivity Analysis of Model Output. Proc. 4th International Conference on Sensitivity Analysis of Model Output (SAMO 2004)*, Hanson et al., Eds., Los Alamos National Laboratory, Los Alamos, USA, 297–230.
- Ganopolski, A., V. Petoukhov, S. Rahmstorf, V. Brovkin, M. Claussen, A. Eliseev, and C. Kubatzki, 2001: CLIMBER-2: A climate system model of intermediate complexity. Part II: Model sensitivity. *Climate Dyn.*, **17**, 735–751.
- Goswami, B. N., V. Venugopal, D. Sengupta, M. S. Madhusoodanan, and P. K. Xavier, 2006: Increasing trend of extreme rain events over India in a warming environment. *Science*, **314**(5804), 1442–1445.
- Hahn, D. G., and J. Shukla, 1976: An apparent relationship between Eurasian snow cover and Indian monsoon rainfall. *J. Atmos. Sci.*, **33**(12), 2461–2462.
- Hansen, J., G. Russell, D. Rind, P. Stone, A. Lacis, S. Lebedeff, R. Ruedy, and L. Travis, 1986: Efficient three-dimensional global models for climate studies: Models I and II. *Mon. Wea. Rev.*, **11**(4), 609–662.
- Haywood, J., 1997: Transient response of a coupled model to estimated changes in greenhouse gas and sulfate concentrations. *Geophys. Res. Lett.*, **24**(11), 1335–1338.
- Ingber, L., 1996: Adaptive simulated annealing (asa): Lesson learned. *Control and Cybernetics*, **25**(1), 33–54.
- IPCC, 2001: *Climate Change 2001: The Scientific Basis. Contribution of Working Group I to the Third Assessment Report of the Intergovernmental Panel on Climate Change*. Cambridge University Press, Cambridge, United Kingdom and New York, NY, USA, 944pp.
- Kalnay, E., and Coauthors, 1996: The NMC/NCAR 40-year reanalysis project. *Bull. Amer. Meteor. Soc.*, **77**, 437–471. [Data available at <http://www.cdc.noaa.gov/>.]
- Kitoh, A., S. Yukimoto, A. Noda, and T. Motoi, 1997: Simulated changes of the Asian summer monsoon at times of increased CO<sub>2</sub>. *J. Meteor. Soc. Japan*, **75**(6), 1019–1031.
- Kripalani, R. H., A. Kulkarni, S. S. Sabade, and M. L. Khandekar, 2003: Indian monsoon variability in a global warming scenario. *Natural Hazards*, **29**(2), 189–206.
- Kripalani, R. H., J. H. Oh, A. Kulkarni, S. Sabade, and H. S. Chaudhari, 2007: South Asian summer monsoon precipitation variability: Coupled climate model simulations and projections under IPCC AR4. *Theor. Appl. Climatol.*, **90**(3–4), 133–159.
- Krishnamurthy, V. and B. N. Goswami, 2000: Indian Monsoon-ENSO relationship on interdecadal timescale. *J. Climate*, **13**, 579–595.
- Kucharski, F., F. Molteni, and J. H. Yoo, 2006: SST forcing of decadal Indian Monsoon rainfall variability. *Geophys. Res. Lett.*, **33**(3), L03709.
- Liu, X., and Z. Yin, 2002: Sensitivity of East Asian monsoon climate to the uplift of the Tibetan Plateau. *Palaeogeography, Palaeoclimatology, Palaeoecology*, **183**, 223–245.
- MAIRS, 2006: MAIRS initial science plan. [Available online from <http://www.mairs-essp.org/lcontent.asp?cid=18&id=47>.]
- May, W., 2002: Simulated changes of the Indian summer monsoon under enhanced greenhouse gas conditions in a global time-slice experiment. *Geophys. Res. Lett.*, **29**(7), 1118–1121.
- Meehl, G., W. Washington, D. Erickson III, B. Briegleb, and P. Jaumann, 1996: Climate change from increased CO<sub>2</sub> and direct and indirect effects of sulfate aerosols. *Geophys. Res. Lett.*, **23**(25), 3755–3758.
- Meehl, G. A., 1994: Coupled land-ocean-atmosphere processes and South Asian monsoon variability. *Science*, **266**, 263–267.
- Meehl, G. A., and W. M. Washington, 1993: South Asian monsoon variability in a model with doubled atmospheric carbon dioxide concentration. *Science*, **260**, 1101–1104.
- Mitchell, J., T. Johns, J. Gregory, and S. Tett, 1995: Climate response to increasing levels of greenhouse gases and sulfate aerosols. *Nature*, **376**, 501–504.
- Morris, M. D., 1991: Factorial sampling plans for preliminary computational experiments. *Technometrics*, **33**(2), 161–174.
- Paeth, H., A. Scholten, P. Friederichs, and A. Hense, 2008: Uncertainties in climate change prediction: El Niño–Southern Oscillation and monsoons. *Global and Planetary Change*, **60**, 265–288.
- Parthasarathy, B., K. Rupa Kumar, and A. Munot, 1992: Forecast of rainy season foodgrain production based on monsoon rainfall. *Indian Journal of Agricultural Sciences*, **62**, 1–8.
- Parthasarathy, B., A. A. Munot, and D. R. Kothawale, 1995: All India monthly and seasonal rainfall series: 1871–1993. *Theor. Appl. Climatol.*, **49**, 217–224.
- Patra, P. K., S. K. Behera, J. R. Herman, S. Maksyutov, H. Akimoto, and T. Yamagata, 2005: The Indian summer monsoon rainfall: interplay of coupled dynamics, radiation and cloud microphysics. *Atmospheric Chemistry and Physics*, **5**, 2181–2188.
- Petoukhov, V., A. Ganopolski, V. Brovkin, M. Claussen, A. Eliseev, C. Kubatzki, and S. Rahmstorf, 2000: CLIMBER-2: A climate system model of intermediate complexity. Part I: Model description and performance for present climate. *Climate Dyn.*, **16**, 1–17.
- Petoukhov, V., A. Ganopolski, and M. Claussen, 2003: POTSDAM—A set of atmosphere statistical-dynamical models: Theoretical background. Technical Report 81, Potsdam Institute for Climate Impact Research, Potsdam. [Available online from [http://www.pik-potsdam.de/publications/pik\\_reports](http://www.pik-potsdam.de/publications/pik_reports).]
- Robock, A., M. Mu, K. Vinnikov, and D. Robinson, 2003: Land surface conditions over Eurasia and Indian summer monsoon rainfall. *J. Geophys. Res.*, **108**(D4), 4131.

- Roeckner, E., L. Bengtsson, J. Feichter, J. Lelieveld, and H. Rodhe, 1999: Transient climate change simulations with a coupled Atmosphere–Ocean GCM including the tropospheric sulfur cycle. *J. Climate*, **12**, 3004–3032.
- Rosenfeld, D., 2000: Suppression of rain and snow by urban and industrial air pollution. *Science*, **287**, 1793–1796.
- Saltelli, A., S. Tarantola, F. Campolongo, and M. Ratto, 2004: *Sensitivity Analysis in Practice. A Guide to Assessing Scientific Models*. John Wiley & Sons, 232pp.
- SimEnv, 2006: A multi-run simulation environment for quality assurance and scenario analyses. [Available online from <http://www.pik-potsdam.de/software/simenv>.]
- Webster, P. J., and S. Yang, 1992: Monsoon and ENSO: Selectively interactive systems. *Quart. J. Roy. Meteor. Soc.*, **118**, 877–926.
- Webster, P. J., V. O. Magaña, T. N. Palmer, J. Shukla, R. A. Tomas, M. Yanai, and T. Yasunari, 1998: Monsoons: Processes, predictability, and the prospects for prediction. *J. Geophys. Res.*, **103**, 14451–14510.
- Zickfeld, K., 2004: Modelling large-scale singular climate events for Integrated Assessment. Ph. D. dissertation, Universität Potsdam, Germany. [Available online from <http://deposit.ddb.de/cgi-bin/dokserv?idn=971983453>.]
- Zickfeld, K., B. Knopf, V. Petoukhov, and H.-J. Schellnhuber, 2005: Is the Indian summer monsoon stable against global change? *Geophys. Res. Lett.*, **32**, L15707. doi: 10.1029/2005GL022771.
- Zwiers, F. W., and V. V. Kharin, 1998: Changes in the extremes of the climate simulated by CCC GCM2 under CO<sub>2</sub> doubling. *J. Climate*, **11**(9), 2200–2222.